Cellular/Molecular

Heterotrimeric G Protein Subunit Gγ13 Is Critical to Olfaction

Feng Li,[1] Samsudeen Ponissery-Saidu,[1] Karen K. Yee,[1] Hong Wang,[1] Meng-Ling Chen,[1,2] Naoko Iguchi,[1] Genhua Zhang,[1,2] Ping Jiang,[3] Johannes Reisert,[1] and Liquan Huang[1]

[1]Monell Chemical Senses Center, Philadelphia, Pennsylvania 19104, [2]Sensory Science Laboratory, School of Bioscience and Food Engineering, Changshu Institute of Technology, Changshu, Jiangsu 215000, China, and [3]The Wistar Institute, Philadelphia, Pennsylvania 19104

The activation of G-protein-coupled olfactory receptors on the olfactory sensory neurons (OSNs) triggers a signaling cascade, which is mediated by a heterotrimeric G-protein consisting of α, β, and γ subunits. Although its α subunit, Gαolf, has been identified and well characterized, the identities of its β and γ subunits and their function in olfactory signal transduction, however, have not been well established yet. We, and others, have found the expression of Gγ13 in the olfactory epithelium, particularly in the cilia of the OSNs. In this study, we generated a conditional gene knock-out mouse line to specifically nullify Gγ13 expression in the olfactory marker protein-expressing OSNs. Immunohistochemical and Western blot results showed that Gγ13 subunit was indeed eliminated in the mutant mice's olfactory epithelium. Intriguingly, Gαolf, β1 subunits, Ric-8B and CEP290 proteins, were also absent in the epithelium whereas the presence of the effector enzyme adenylyl cyclase III remained largely unaltered. Electro-olfactogram studies showed that the mutant animals had greatly reduced responses to a battery of odorants including three presumable pheromones. Behavioral tests indicated that the mutant mice had a remarkably reduced ability to perform an odor-guided search task although their motivation and agility seemed normal. Our results indicate that Gαolf exclusively forms a functional heterotrimeric G-protein with Gβ1 and Gγ13 in OSNs, mediating olfactory signal transduction. The identification of the olfactory G-protein's βγ moiety has provided a novel approach to understanding the feedback regulation of olfactory signal transduction pathways as well as the control of subcellular structures of OSNs.

Introduction

The ability to sense olfactory cues is important to an animal's survival and reproduction. In rodents and other vertebrates, odorants are mostly detected by the olfactory sensory neurons (OSNs) residing in the main olfactory epithelium in the nasal cavity. Most OSNs express one of hundreds of G-protein-coupled olfactory receptors (ORs) (Buck and Axel, 1991; Glusman et al., 2001; Young et al., 2002; Zhang and Firestein, 2002; Mombaerts, 2004; Munger et al., 2009; Ma, 2010). Activation of these ORs leads to the dissociation of a heterotrimeric G-protein, Golf, into α and βγ moieties. The dissociated α subunit, Gαolf (Jones and Reed, 1989), stimulates an effector enzyme, adenylyl cyclase III (ACIII) (Bakalyar and Reed, 1990), which produces the second messenger cAMP, thus opening the olfactory cyclic nucleotide-gated (CNG) ion channel (Dhallan et al., 1990; Bradley et al., 1994; Liman and Buck, 1994; Bonigk et al., 1999), leading to the influx of Na^+ and Ca^{2+} ions and depolarizing the membrane potential. The depolarization is further augmented by the efflux of Cl^- via a Ca^{2+}-gated chloride channel (Kleene, 1993; Lowe and Gold, 1993; Stephan et al., 2009), which eventually triggers the generation of action potentials that propagate along the axon to the axon terminus in the olfactory bulb.

Although several of important OR-mediated signaling components have been identified, some key elements including the Gαolf's βγ partners remain to be fully established. Recent studies have shown that Gβγ subunits are not just the binding partners of the Gα subunits, but also regulate many effectors including adenylyl cyclases, phospholipases, protein kinases, ion channels, and histone deacetylases (Spiegelberg and Hamm, 2005; Dupre et al., 2009), contributing to the regulation of olfactory signal transduction as well as control of gene expression in OSNs (DeMaria and Ngai, 2010). Thus, it seems necessary to identify Gαolf's βγ subunits to fully understand the molecular processes of mammalian olfactory system.

We and others have reported the expression of at least two Gγ subunits in the main olfactory epithelium: Gγ8 and Gγ13 (Tirindelli and Ryba, 1996; Huang et al., 1999). The former, however, is expressed more strongly in the developing olfactory epithelium and at a reduced level in the mature epithelium, suggesting that it is more likely involved in the development of the olfactory system. In contrast, Gγ13 is found in the cilia layer of the mature olfactory epithelium, but absent in the cilia layer of certain anosmic disorders, implicating its possible role in olfac-

Received Dec. 4, 2012; revised March 20, 2013; accepted March 30, 2013.

Author contributions: F.L., S.P.-S., K.K.Y., H.W., M.-L.C., P.J., J.R., and L.H. designed research; F.L., S.P.-S., K.K.Y., H.W., M.-L.C., N.I., G.Z., P.J., J.R., and L.H. performed research; F.L., S.P.-S., K.K.Y., H.W., P.J., J.R., and L.H. analyzed data; S.P.-S., K.K.Y., H.W., P.J., J.R., and L.H. wrote the paper.

This work was support by NIH Grants R01DC007487 (L.H.), R01DC009613 (J.R.), and DC010012 (H.W.), and a core facility Grant P30 DC011735 (R. Margolskee in support of Monell Core Facilities), and from National Science Foundation Equipment Grant DBI-0216310 (N. Rawson in support of Monell's Confocal Microscopy), and from National Natural Science Foundation of China Grant 31228008 (L.H.). We thank Drs. Jiang Xu, Robert Margolskee, and Charles Wysocki for helpful discussion, and Minliang Zhou for technical support.

The authors declare no competing financial interests.

Correspondence should be addressed to Dr. Liquan Huang, Monell Chemical Senses Center, 3500 Market Street, Philadelphia, PA 19104. E-mail: lhuang@monell.org.

DOI:10.1523/JNEUROSCI.5563-12.2013

 0270-6474/13/337975-10$15.00/0

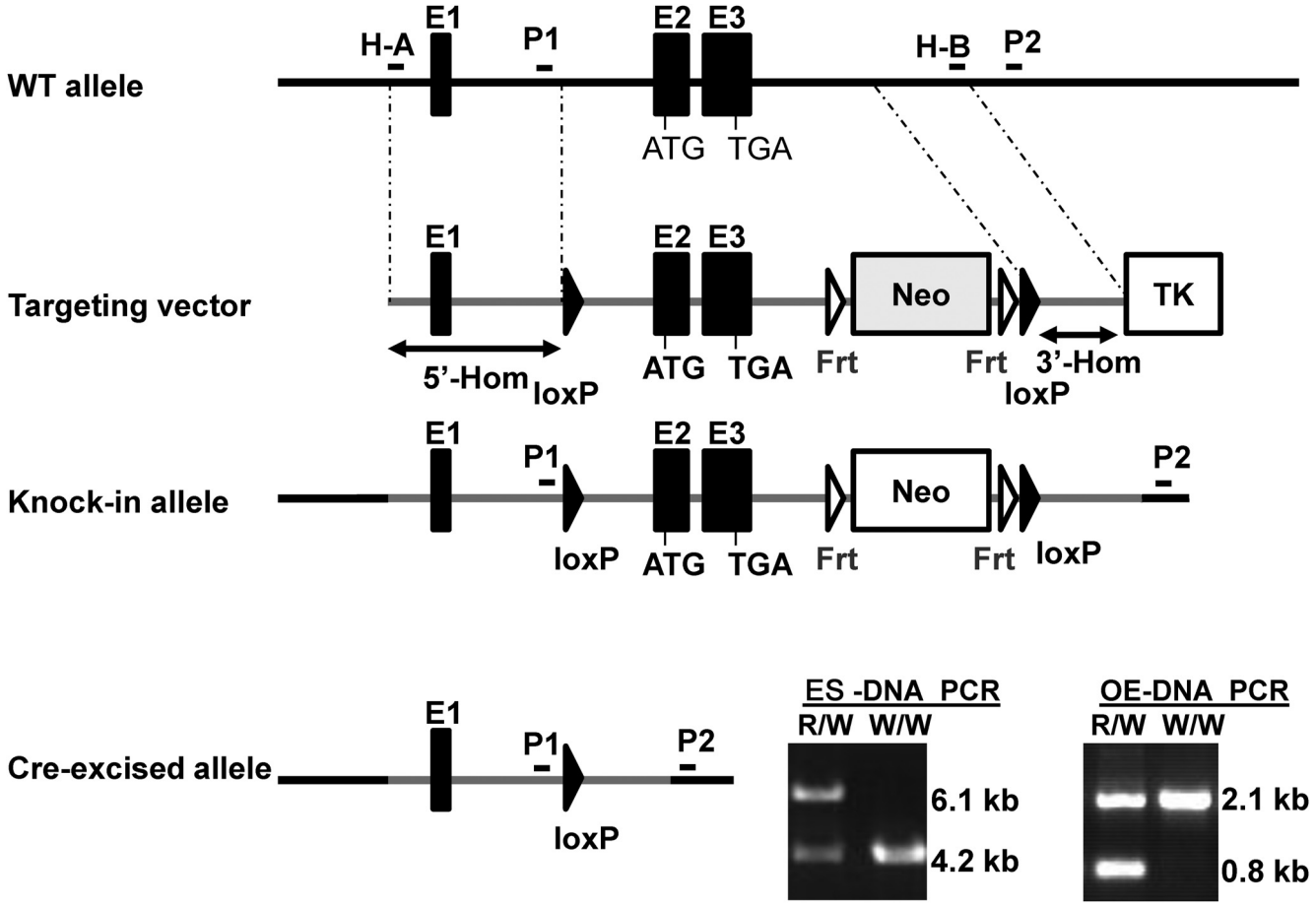

Figure 1. Targeted disruption of the *Gng13* gene. The wild-type (WT) allele of the gene consists of three exons: E1, E2, and E3, with the start codon ATG in E2 and the stop codon TGA in E3. The entire *Gng13* gene was translocated into the targeting vector by homologous recombination in the *Escherichia coli* cells through two flanking homologous sequences: H-A and H-B. The same recombination approach was used to insert a loxP site and a Frt-Neo-Frt-loxP cassette into intron 1 and 3′-end sequence downstream of exon 3, respectively, which is followed by the thymidine kinase gene (TK) on the targeting vector for embryonic stem (ES) cell counter-selection. The recombination at the 5′- and 3′- homologous arms (5′-, 3′-Hom) in the mouse ES cells resulted in the generation of the knock-in allele, which was identified by PCR screening with the two primers P1 and P2 located upstream of the first loxP site and downstream of 3′-Hom, respectively. DNA templates prepared from the ES cells containing both the recombinant and WT alleles (ES-DNA PCR inset: R/W lane) produced two PCR products of 6.1 and 4.2 kb, whereas that containing only WT allele generated a single amplified product of 4.2 kb (W/W lane). In the olfactory sensory neurons that express Cre recombinases, the sequence between two loxP sites was excised, deleting all coding exons of the *Gng13* gene, and PCR with P1 and P2 primers and genomic DNA from this olfactory epithelium generated two PCR products of 0.8 kb from the excised allele and 2.1 kb from WT allele (OE-DNA PCR inset: R/W lane), whereas genomic DNA from WT olfactory epithelium generated a single amplified product of 2.1 kb (W/W lane).

tory signal transduction (Kulaga et al., 2004; McEwen et al., 2007; Kerr et al., 2008). To elucidate the role of Gγ13 in the olfactory signal transduction, we generated a genetically engineered mouse with two loxP sites flanking the only two coding exons of the Gγ13's gene, *Gng13*, and crossed this mouse with another transgenic mouse (OMP^{Cre}) that expresses Cre recombinases under the promoter of the olfactory marker protein gene (*Omp*) in the mature OSNs (Li et al., 2004). Molecular, immunohistochemical, electrophysiological, and behavioral data suggested that Gγ13 forms a functional G-protein with Gβ1 and Gαolf that is critical to mammalian olfaction.

Materials and Methods

Animals

All studies involving animals were performed according to protocols approved by the Monell Chemical Senses Center Institutional Animal Care and Use Committee. Mice were housed in a climate-controlled environment at the Animal Care Facility of the Monell Chemical Senses Center.

Reagents

Antibodies. Rabbit polyclonal antibodies against Gαolf (sc-386), Gβ1 (sc-379), Ric-8B (sc-109013), and ACIII (sc-588) were purchased from Santa Cruz Biotechnology, and goat antibody against OMP from Wako Chemicals, anti-CEP290 from Bethyl Laboratories, and mouse monoclonal antibodies again acetylated tubulin and β-actin from Sigma-Aldrich. The generation of the antibody against Gγ13 was previously described (Huang et al., 1999). Alexa 488-conjugated goat-anti-rabbit, goat-anti-mouse and donkey-anti-goat secondary antibodies were purchased from Life Technologies.

Odorants. Heptanal, eugenol, amyl acetate, acetophenone, geraniol, cineole, decanal, hexanal, isovaleric acid, 2-heptanone, 2, 5 dimethyl pyrazine (DMP), citral, and triethylamine (TEA) were obtained from Sigma-Aldrich. Lilial and 2, 5-Dihydro-2, 4, 5 trimethylthiazoline (TMT) were obtained from International Flavors and Fragrances and Contech, respectively.

Generation of the conditional knock-out mice

To prepare the conditional knock-out construct, the bacteriophage λ red protein-based recombination system was used to generate the targeting vector (Liu et al., 2003). Briefly, a bacterial artificial chromosome (BAC) clone, RP24-277M16, that contains the entire Gγ13 gene *Gng13*, was ordered from the Children's Hospital Oakland-BACPAC Resources (http://bacpac.chori.org/). The BAC clone was used as a template for PCR amplification of the two mini-homology arms, H-A (379 bp) and H-B (416 bp), that flank the *Gng13* gene (Fig. 1). The following PCR primers for H-A and H-B were restriction enzyme sites attached: for

H-A, forward, NotI-H-AF (ATAAGCGGCCGCAAGAGTTGCCTTGG TCATG), and reverse, HindIII-H-AR (GTCAAGCTTGAGGTAGCCGT GTAATCAGT); for H-B, forward, HindIII-H-BF(GTCAAGCTTTACCC CATACTCAACACCC), and reverse, SpeI I-H-BR, (TCTACTAGTG GT GGGTTCCAAAGTAAAG). The two mini-arms were subcloned into a pBluescript-based vector, PL253, at the NotI and SpeI I sites upstream of the MCI thymidine kinase (TK) gene (Liu et al., 2003). The intermediate vector PL253-H-A-B was linearized and electroporated into SW106 cells that harbored the BAC clone RP24-277M16 to retrieve the 11 kb genomic DNA encompassing the *Gng13* gene from the BAC DNA using the gap repair method. Recombination at H-A and B between the linearized vector and the BAC DNA led to the generation of a circular plasmid PL253Gng13 containing the targeted 11 kb DNA.

To introduce a loxP site into the first intron of the *Gng13* in the plasmid PL253Gng13, two homology mini-arms H-C and D were produced by PCR amplification from the intron using the restriction enzyme sites-attached PCR primers: for H-C, forward, NotI-H-CF (ATAAGCGGCCGCTCTCAC TGGTTCCTTGCGA), and reverse, EcoRI-BglII-H-CR (GTCGA ATTCA GATCTGAGGCTGAGAGGCCAAGTT); for H-D, forward, BamHI-H-DF (ATAGGAT CCAGGCAGCACCCAGCATCTC), and reverse, SalI-H-DR (GTCGTCGACCACCCATTGGT CCTTCCTGA). These mini-arms were ligated with a floxed neomycin resistance cassette (loxP-Neo-loxP) from the plasmid PL452 to construct a mini-targeting vector pBluescript-H-C-loxP-Neo-loxP-H-D. The loxP-Neo-loxP cassette was introduced into the PL253Gng13 vector by the same gap repair method. The induction of Cre expression in the SW106 cells removed the Neo cassette but left one loxP site and an engineered BamH I site from the H-D mini-arm.

The same gap repair approach was used to introduce an Frt-Neo-Frt-loxP cassette from the plasmid PL451 into the 3′ end of the *Gng13* gene with homology mini-arms H-E and F, which were produced by PCR amplification with the restriction enzyme sites-attached primers: for H-E, forward, NotI-H-EF (ATAAGCGGCCGCCCGAACAGCATTTG AGAC), and reverse, EcoRI-H-ER (GTCGAATTCGGAGCAAGATGA TTACCG); for Hom F, forward, BamHI-H-FF (ATAGGATCCCACAC ACACACCTGCTCC), and reverse, SalI-H-FR (GTCGTCGACTATCT TGCCTCACCCACCT).

The final targeting vector (Fig. 1), which contained one loxP sequence in the first intron and the Frt-Neo-Frt-loxP cassette at the 3′-end with the 5′- and 3′-homology arms of 7.2 and 2.3 kb (5′-, 3′-Hom), respectively, was verified by sequencing analysis, and linearized by NotI digestion, and electroporated into 129S4/SvJae-derived J1 embryonic stem (ES) cells (Jiang et al., 2002). These ES cells were selected with G418 at 400 μg/ml and ganciclovir at 2 μM. Approximately 240 ES cell clones were obtained and expanded in 24-well plates. Genomic DNA was prepared from each clone and used for PCR screening with the two primers corresponding to the sequence immediately upstream of the first loxP site (P1: ACATAC CCCACCCTACATGCAA) or to the mouse genomic sequence downstream of H-B (P2: ATGCAGAATGTGGCTAGGATG) (Fig. 1). The PCR product from the clones with the correct knock-in allele was 6.1 kb, whereas that from the WT allele was 4.2 kb (Fig. 1, inset) (ES-DNA PCR), and the PCR products were confirmed by sequencing analysis.

Genomic DNA samples from two of the 240 colonies generated the correct PCR product. These two colonies were further expanded and microinjected into C57BL/6J blastocysts. Eight chimeric male mice were obtained with chimerism ranging from 50 to 95%. These mice were bred with C57BL/6J female mice to generate F1 progeny, which were genotyped with two pairs of PCR primers: one covering the first loxP sequence (loxP1F, GCAGCCCAATTCCGATCATA and loxp1R, GGGCAAATGA GCCTGAGAAGG), generating a 0.27 kb product from the knock-in or no product from WT alleles, respectively, and the other covering the Frt-Neo-Frt-loxP cassette (cassette F: CACGTCCAAAGAAGTCCCTC TCAGGC and cassette R: CCTTGGCTAGCCGACTCTCA), generating 2.3 and 0.4 kb products from the knock-in and WT alleles, respectively.

To abolish Gγ13 expression in the olfactory epithelium, the newly engineered mouse carrying the floxed *Gng13* gene was crossed with another gene knock-in mouse (OMP^{Cre}), in which the OMP coding sequence was replaced by the coding sequence for Cre, thus expressing Cre recombinases in the mature OSNs (Li et al., 2004). To minimize possible effects resulting from the *Omp* gene nullification (Buiakova et al., 1996; Youngentob and Margolis, 1999; Youngentob et al., 2001; Reisert et al., 2007; Kwon et al., 2009; Lee et al., 2011), in this study, only the OMP^{Cre} heterozygotes were used so that all mice had one *Omp* allele intact. To determine the Gγ13's contribution to olfaction, adult male and female mice of all three genotypes: homozygous knock-out ($Gng13^{-/-}$), heterozygotes ($Gng13^{+/-}$), and wild-type control ($Gng13^{+/+}$) were used, which had mixed genetic background of ~87.5% of C57BL/6J and 12.5%129. To verify whether the floxed *Gng13* exons 2 and 3 could be excised by the OMP-Cre, genomic DNA was prepared from the $Gng13^{+/-}$ olfactory epithelium with one *Omp* allele replaced by OMP^{Cre}. PCR with the P1 and P2 primers detected 0.8 kb product from the excised allele (Fig. 1, inset) (OE-DNA PCR), and sequencing analysis of the PCR product confirmed the recombination.

Immunohistochemistry

WT and KO ($Gng13^{-/-}$) mice were anesthetized and cardiacally perfused with 4% paraformaldehyde in PBS. The olfactory organs were dissected out and postfixed for 2 h, and then decalcified in 250 mM EDTA in PBS for 2 d. Tissues were cryoprotected in 20% sucrose. Coronal sections of 12 μm thickness were sliced and immunostained following standard immunohistochemistry procedures. Briefly, sections were blocked in the blocking buffer (3% BSA, 0.3% Triton X-100, 2% goat or horse serum, and 0.1% sodium azide in PBS), and then incubated with rabbit antibodies against Gγ13 (Huang et al., 1999), Gαolf, Gβ1, and ACIII, mouse monoclonal antibody against acetylated tubulin, and goat antibody against OMP. Immunosignal was visualized using an Alexa488-conjugated goat-anti-rabbit, goat-anti-mouse, or donkey-anti-goat secondary antibodies, respectively. Images were taken using a Leica TCS SP2 spectral confocal microscope.

Western blot analysis

To characterize the effect of *Gng13*-KO on the expression of other olfactory signaling proteins and Gγ13-interacting proteins, WT and KO olfactory epithelia were lysed in Laemmli sample buffer (Bio-Rad) with β-mercaptoethanol and protein samples were prepared for SDS-PAGE and then transferred to polyvinylidene difluoride membrane as previously described (Wang et al., 2007). Western blots were first incubated with antibodies against Gγ13, Gβ1, Ric-8B, CEP290, ACIII, OMP, and β-actin, followed by horseradish peroxidase-conjugated anti-rabbit, anti-goat, or anti-mouse secondary antibodies. The signals were detected with an enhanced chemiluminescence detection system (ECL Western Blotting Analysis System, GE Healthcare), and quantified using Alpha-EaseFC/Alpha Imager 2000 software (Alpha Innotech).

Quantitative real-time PCR analysis

Total RNA was extracted using Absolutely RNA Microprep kit (Agilent Technologies) from WT and KO ($Gng13^{-/-}$) olfactory epithelia. An approximately equal amount of total RNA from each animal was reverse transcribed into cDNA using Superscript III reverse transcriptase (Life Technologies). Power SYBR Green PCR Master Mix (Life Technologies) was used to set up real-time PCRs, which were run in an ABI PRISM 7000 Sequence Detection System (Life Technologies). The specificity of the PCRs was analyzed by dissociation studies using the instrument's program and confirmed by DNA sequence analysis. The relative gene expression levels were determined using the $2^{-\Delta\Delta Ct}$ method, which normalizes the expression levels of genes of interest against those of "housekeeping" genes (β-actin) in the same sample and compares the expression levels among WT and KO samples as previously described (Wang et al., 2007). Real-time PCR primers were designed to have nearly the same annealing temperature: (1) Gγ13's gene *Gng13*: forward, CTGCTTTTGCTGTCTC CTCC; reverse, AGGCCAGTTGGTACTTGAGG; Gαolf's gene *Gnal*: forward, GAGAACCAGTTCCGGTCAGA; reverse, CTCAAAGCAGGC CTTCACTC; Gβ1's gene *Gnb1*: forward, CTCCTCCTTGCTGGGTAT GA; reverse; AAGC AGCTGACTCGGTTGTC; ACIII's gene *Adcy3*: forward, CAGCAG GATGAGCTGGAAG; reverse, ACATGATGCCCACG ATGATA; OMP's gene *Omp*: forward, AACAACTCTAGC CACCCACG; reverse, ACCTCCACCAAGTCCACAAG.

Air-phase electro-olfactogram recordings

The recording setup and procedure were essentially similar to that described previously (Cygnar et al., 2010). Briefly, mice were killed using

CO_2 followed by decapitation and the head was bisected sagitally along the midline, and the nasal septum was removed to expose the endoturbinates 2, 2b, 3, and 4. For all electro-olfactogram (EOG) recordings, the right hemi-head was used. The hemi-head was placed on a recording dish and was exposed to a continuous stream of humidified air at a flow rate of 3 L/min. Odorant solutions were made by dissolving stock solutions in DMSO into 5 ml of H_2O at a final concentration of 0.1 M, which were stored in glass vials with silicone stoppers and allowed to equilibrate for at least 30 min before being used for experiments.

Odorants and pheromones were applied using pressure pulses (10 psi, 100 ms) delivered by a picospritzer III system (Parker Hannifin). A set of 15 odorants in the order shown in Figure 6 was used to elicit and record responses from endoturbinates 2 and 2b. Heptanal (0.1 M) was used between sets of stimuli to monitor the response consistency of the olfactory epithelium over time. The odorants were applied at an interval of 1 min. Blanks consisted of 2% DMSO in H_2O (v/v). Heptanal (0.1 M) was used to survey the surface of the four visible turbinates (2, 2b, 3, and 4) for responses in the WT and KO mice. Recordings were made using two recording electrodes and a ground electrode connected to two Warner DP-301 amplifiers. The 1 kHz low-pass signal was digitized using CED Micro 1401 mkII digitizer and was fed to a PC. Signal Ver.5.01 (CED) was used to acquire the data at a sampling rate of 2 kHz.

Behavioral tests

The experiments were performed following the previously published procedures with minor modifications (Luo et al., 2002). Briefly, for the buried food-seeking tests, mice at ≥6-weeks-old were deprived of food for 24 h. On day 2, a 1 g pellet of regular chow was scented with 5 μl of 10% peanut butter dissolved in mineral oil, and buried ~1 cm beneath the surface of fresh bedding at one end of a clean test cage of a regular size (24 cm length ×14 cm width × 13 cm height), and the bedding surface was smoothed out. The mouse was transferred from its home cage and released at the other end of the test cage. The time from its introduction to the test cage until it found the food pellet and started to eat was recorded as the latency. If an animal could not find the food pellet within 10 min, the test was terminated and the latency was recorded as 600 s. The procedure for the unburied food-seeking tests was the same except that the food pellet was placed on the surface of the bedding.

Data analysis

Real-time PCR data, physiological response amplitudes, or behavioral scores were grouped and averaged according to the genotypes. Pairwise comparisons of the averaged numbers were analyzed using two-way ANOVA and Student's *t* tests. A P value < 0.05 was the criterion for statistical significance.

Results

Conditional nullification of the mouse olfactory Gγ13 expression

The gene coding for Gγ13, *Gng13*, consists of three exons, with the start codon in the second exon and stop codon in the third exon. Previous studies have shown that Gγ13 is expressed not only in the chemosensory organs but also in the CNS and other tissues (Huang et al., 1999; Kulaga et al., 2004; Kerr et al., 2008). To ablate Gγ13 expression in the olfactory epithelium only, we generated a genetically modified mouse with *Gng13* gene's second and third exons floxed (Fig. 1). The first loxP site was introduced at 413 bp upstream of the second exon, whereas the second loxP site along with a flippase recognition target (Frt) sequence-neomycin resistance gene-Frt cassette for embryonic cell selection was introduced at 541 bp downstream of the third exon. The targeting DNA was electroporated into mouse ES cells. Of 240 ES cell colonies screened for the recombination between the genomic DNA and homologous arms on the targeting DNA, two of them contained the correct integrations, which were expanded and then injected into C57BL/6J blastocysts and transferred to surrogated mothers. Eight chimeric male mice were obtained with chimerism of 50–95%, and bred with C57BL/6 mice for two more generations before crossing with another knock-in mouse OMP^{Cre} that expresses Cre recombinases in the mature OSNs (Li et al., 2004), thus excising the floxed second and third exons of the *Gng13* gene and abolishing Gγ13 subunit synthesis in these cells.

The KO ($Gng13^{-/-}$) mice appeared to be grossly normal, although survival of newborns was compromised in litters of seven or more pups. The Cre sequence also disrupts the OMP coding sequence in this OMP^{Cre} knock-in mouse, and the disruption of OMP expression can also affect the mutant animals' physiological and behavioral responses (Buiakova et al., 1996; Youngentob and Margolis, 1999; Youngentob et al., 2001; Reisert et al., 2007; Kwon et al., 2009; Lee et al., 2011). Therefore, in this study, only the heterozygous $OMP^{Cre/WT}$ mice were used so that one intact OMP allele remained in these animals. To examine whether the OMP-Cre was able to excise the floxed *Gng13* exons, PCR was performed with P1 and P2 primers and the genomic DNA prepared from WT and $Gng13^{+/-}$ olfactory epithelia. Products of 0.8 kb from the excised allele as well as 2.1 kb from WT allele were amplified from the $Gng13^{+/-}$ sample, whereas only a single product of 2.1 kb was obtained from WT sample(Fig. 1, inset) (OE-DNA PCR), and sequencing analysis confirmed the predicted recombination.

Altered expression of olfactory signaling molecules in the $Gng13^{-/-}$ olfactory epithelium

To determine how the excision of the two exons of *Gng13* affected the Gγ13 protein expression, immunohistochemistry was performed on the olfactory epithelium from 8-month-old male mice of both $Gng13^{-/-}$ and WT control. The result showed that although the Gγ13 immunoreactivity was abundantly detected in the WT olfactory epithelium, particularly in the cilia layer as well as the nerve bundles beneath the olfactory epithelium, it was absent in the KO epithelium, including the cilia layer (Fig. 2). Some nerve bundles in the KO olfactory tissue section appeared to still express Gγ13, which may originate from cells other than the OSNs or from the OSNs that do not express OMP.

To determine whether the *Gng*13 gene disruption affected other olfactory signaling molecules' expression, we performed immunostaining with the antibodies against Gαolf, Gβ1 and adenylyl cyclase III (ACIII). Interestingly, the results showed that the two G-protein subunits Gαolf and Gβ1 were also absent in the KO epithelium whereas the expression of the effector enzyme ACIII appeared to be strong but its subcellular distribution seemed to have shifted to the cell body (Fig. 2). To determine whether KO affected the cilia structure of the olfactory epithelium or the expression of the OMP itself, we also performed the immunostaining with antibodies against acetylated tubulin and OMP. Strong staining of anti-acetylated tubulin antibody was detected in the cilia layer of both WT and KO (Fig. 2). Similar results were also observed with anti-OMP antibody except that anti-OMP staining was also found in the cell bodies.

To further characterize the expression of the Gγ13 and its interacting proteins in KO olfactory epithelium, we performed Western blot analysis (Fig. 3*A*,*B*). The results showed that Gγ13 protein signals in KO sample were hardly detectable, corresponding to only 1.5% of WT sample; and those of Gβ1, Ric-8B, and CEP290 proteins were much reduced in KO sample, equivalent to 9.1, 6.7, and 23% of those in WT sample, respectively. ACIII protein signals, on the other hand, were comparable to those of

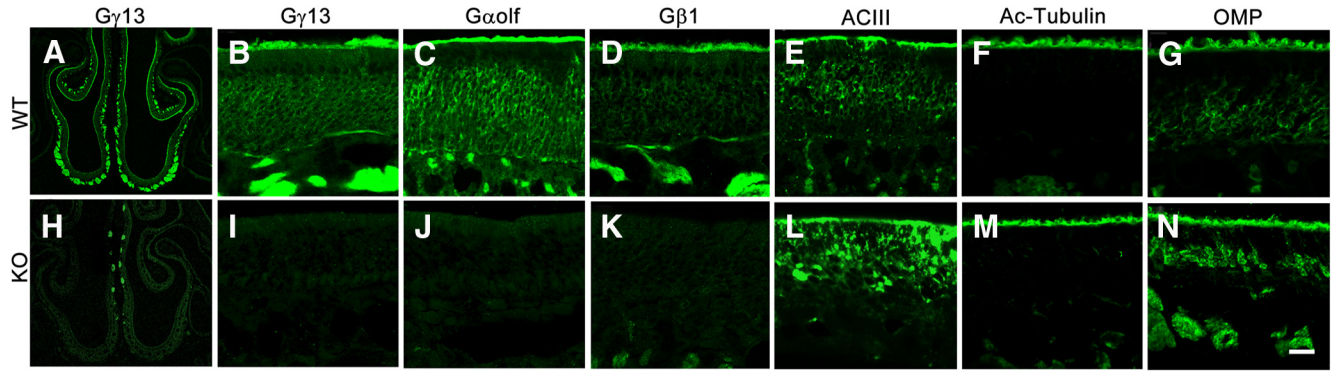

Figure 2. Immunostaining of WT and KO olfactory epithelia with antibodies against olfactory signaling components. Eight-month-old male mice of WT and KO were used for this experiment. Gγ13, Gαolf, Gβ1, ACIII, acetylated tubulin (Ac-Tubulin), and OMP immunostaining on WT (***A–G***) and KO (***H–N***) olfactory epithelium. Scale bar, ***A***, ***H***, 100 μm; ***B–G***, ***I–N***, 25 μm.

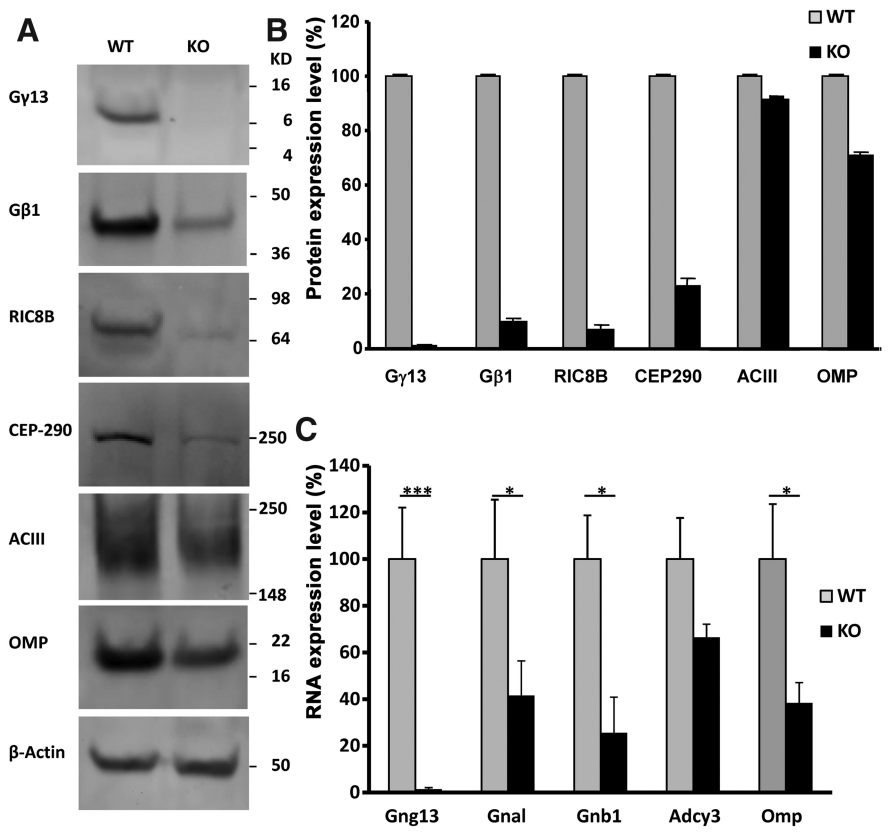

Figure 3. Western blot and real-time PCR analyses of the effect of *Gng13* KO on expression of olfactory proteins. ***A***, Western blots were prepared from lysates of the olfactory epithelia isolated from WT and KO mice, which were incubated with the primary antibodies against Gγ13, Gβ1, Ric-8B(RIC8B), CEP290, ACIII, OMP, and β-Actin, followed by the horseradish peroxidase-conjugated secondary antibodies. ***B***, Plot of signal intensities from Western blots in ***A***. The relative levels of other proteins were normalized against those of β-actin in each sample and then the intensities of other proteins in WT were set to 100 to determine the relative intensities of the corresponding proteins in KO sample. ***C***, Relative transcript levels. As with ***B***, β-actin transcript levels were used as an internal control to normalize other genes' transcript levels in different samples, and WT levels for other genes were set to 100. Error bars represent SEM. ***$p > 0.001$; *$p > 0.05$.

WT, i.e., 91.4% of its WT counterpart whereas OMP signals were somewhat reduced to 70.9% of the WT.

To determine whether the changes in expression of the signaling proteins resulted from altered transcript levels, we also performed quantitative real-time PCR with RNA samples prepared from WT and KO olfactory epithelia (Fig. 3*C*). The results showed that the transcripts of Gγ13, Gαolf, Gβ1, and adenylyl cyclase III as well as OMP (gene symbols: *Gng13*, *Gnal*, *Gnb1*, *Adcy3*, and *Omp*) were reduced to 1.7, 41.6, 25.5, 66.5, and 38.4% of their WT counterparts, respectively.

Absence of Gγ13 subunits in the glomeruli of the *Gng13*$^{-/-}$ mutant mice

To determine whether *Gng13* KO also altered its expression in the axonal termini of the OSNs, immunohistochemistry was performed on olfactory bulb sections. The results indicated that although expression of OMP was detected, Gγ13 immunoreactivity was significantly reduced in KO glomeruli compared with that in WT glomeruli; the axon bundles and the glomerular structures appeared somewhat altered (Fig. 4).

Absence of electro-olfactogram responses of the KO mice to odorants and pheromones

To characterize the effect of *Gng13* gene absence on olfaction at the physiological level, we performed air-phase EOG recordings to compare the odorant/pheromone-evoked electrophysiological responses in the WT and KO olfactory epithelia. An EOG recording is typically a negative-going field potential measured from a point on the surface of the olfactory epithelium which represents the sum of neuronal activity in that region (Ottoson, 1956). We tested 15 odorants, including three that are considered to be pheromones: 2-heptanone, DMP, and TMT (Rodriguez and Boehm, 2009). In WT epithelia, all odorants elicited responses of appreciable amplitudes, although quite different for different odorants or pheromones (Figs. 5, 6*A*). Mean maximal responses of ~−15 mV were obtained with heptanal, amyl acetate, hexanal, and 2-heptanone. However, in KO epithelia, responses were remarkably diminished for all tested odorants (Fig. 6*A*). TEA elicited positive responses in the KO mice, reminiscent of what has been observed for the G_{olf} and CNGA2 knock-outs (Fig. 5) (Brunet et al., 1996;

Belluscio et al., 1998). The positive EOG observed during TEA exposure is thought to result from odorant-evoked mucus-secreting activity of nonneuronal support cells in the epithelium, which is partially masked in the WT by the negative response of OSNs to TEA (Okano and Takagi, 1974).

The responses to the 15 odorants and pheromones were recorded from only two points from the anterior part of endoturbinates 2 and 2b. To exclude the possibility of the presence of responsive regions in other parts of the epithelium in mutant mice, responses to heptanal (0.1 M) were recorded from multiple points on the epithelium (Fig. 6*B*). Whereas in the WT, heptanal elicited responses of robust amplitudes at all the points tested, in the mutant, the response amplitudes remained negligible everywhere.

To determine whether the insertion of loxP sites in the *Gng13* gene affected the olfactory sensation, we also tested the control mice carrying two alleles of floxed *Gng13* with no Cre expression, i.e., *Gng13* $^{fl/fl}$*Omp* $^{w/w}$. The results showed that these mice were capable to generate responses undistinguishable from WT mice (data not shown); indicating that the loxP insertions per se did not alter the olfactory responses.

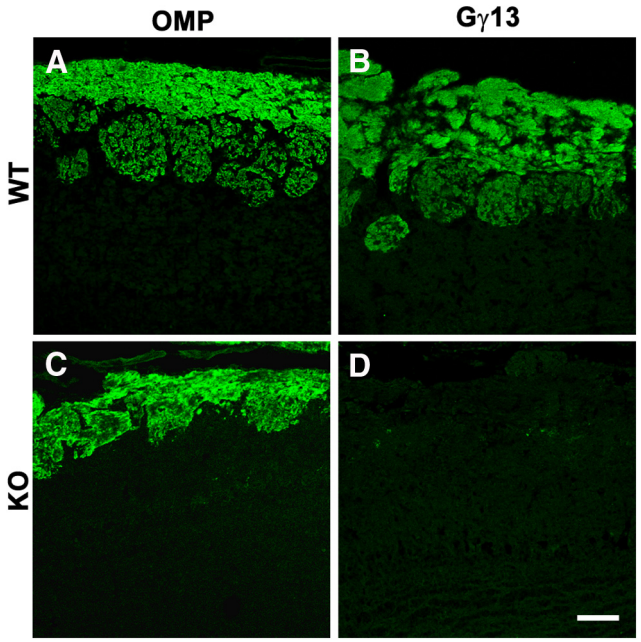

Figure 4. Immunostaining of olfactory bulb sections. While OMP was detected in axon bundles and glomeruli of both WT and KO tissues (***A***, ***C***), Gγ13 immunoreactivity was found only in the WT section (***B***) and not in the KO section (***D***). Scale bar, 80 μm.

Absence of odor-guided food-seeking behavior

To test whether *Gng13* nullification in the OSNs affected the animals' behavioral responses, we performed food-seeking tests following previously published procedures, with minor modifications (Luo et al., 2002; Yang and Crawley, 2009). Sex/age-matched mice were deprived of food for 1 d and then introduced individually into a clean test cage with a 1 g pellet of chow scented with 5 μl of 10% peanut butter buried beneath the fresh bedding. The results showed that the WT and heterozygous (HT, *Gng13* $^{FL/WT}$*Omp* $^{Cre/WT}$) mice took an average of ~27 and 26 s, respectively, to locate the food, whereas the KO mice needed significantly longer (518 s on average) to do the same (Fig. 7). On the other hand, when the food was placed on top of the bedding, it took the WT, HT, and KO mice 10, 11, and 13 s to find the food (Fig. 7).

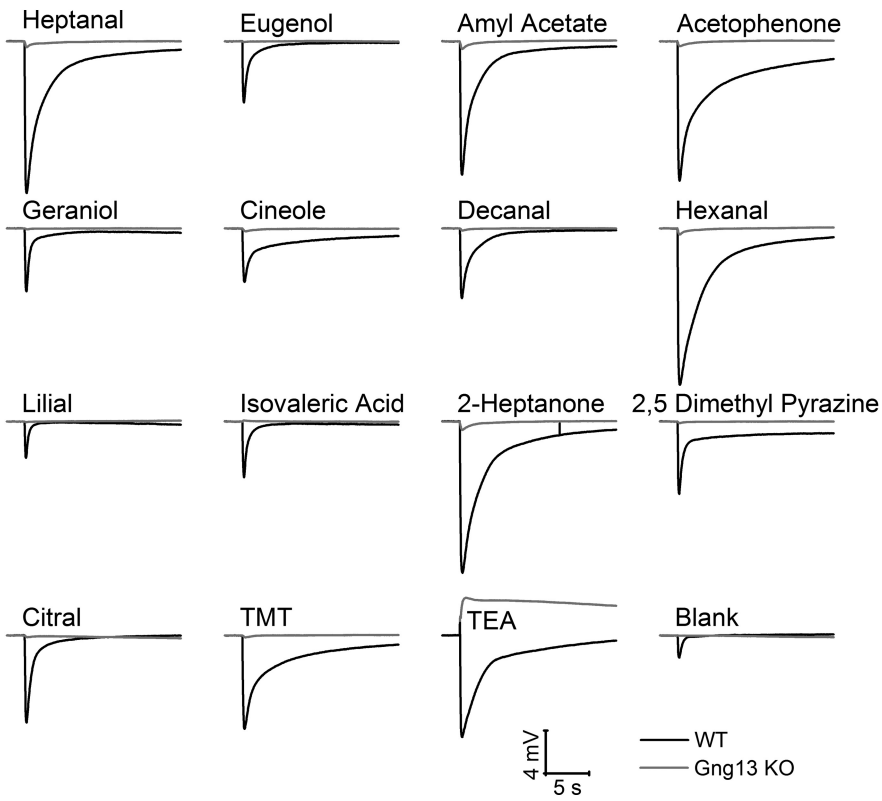

Figure 5. Representative EOG responses from WT and KO mice. *Gng13*-KO epithelia (gray traces) had very small EOG responses to odorants compared with WT epithelia (black traces). All odorants/pheromones were applied for 100 ms at 0.1 M in solution. TEA elicited a biphasic response in WT epithelia and a positive response in KO epithelia.

Discussion

The dominant transduction mechanism in OSNs is a canonical G-protein-coupled pathway where receptor activation leads to a rise in intracellular cAMP via a heterotrimeric G-protein and ACIII activation (Munger et al., 2009; Ma, 2010). cAMP gates a Ca^{2+} permeable heteromeric CNG channel, triggering the opening of a secondary excitatory Ca^{2+} activated Cl^- channel Ano2. A very successful strategy to identify the proteins involved in olfactory transduction and their behavioral relevance has been their genetic ablation. This has been performed for several olfactory transduction proteins, including Gαolf and ACIII (Belluscio et al., 1998; Wong et al., 2000), the three CNG channel subunits and Ano2 (Brunet et al., 1996; Munger et al., 2001; Michalakis et al., 2006; Billig et al., 2011) and proteins responsible for signal transduction termination (OMP and NCKX4) (Buiakova et al., 1996; Stephan et al., 2012). Several G-protein β and γ subunits expressed in OSNs have been iden-

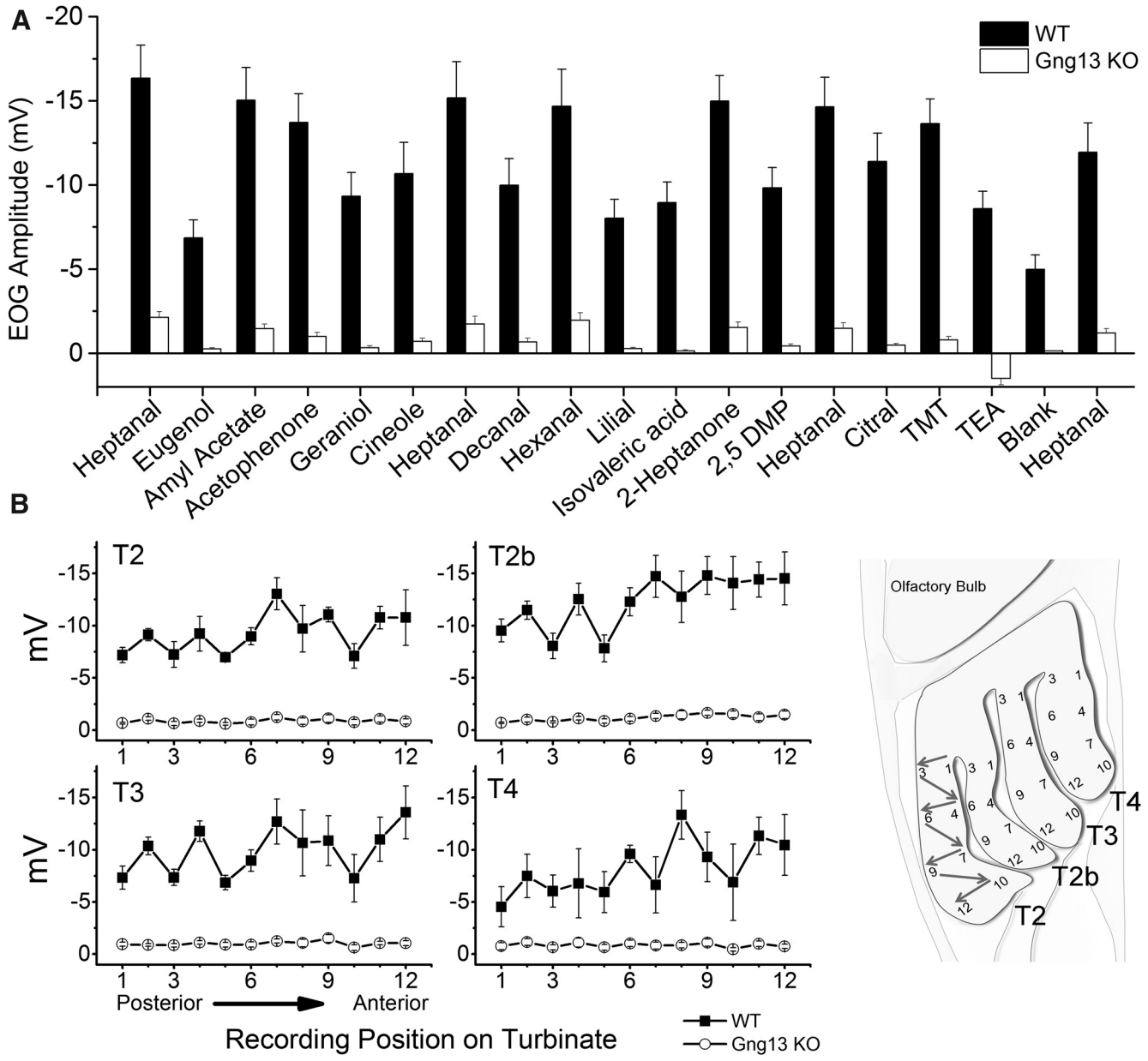

Figure 6. EOG amplitudes to odorants were diminished in *Gng13*-KO epithelia. ***A***, Responses to a set of 15 odorants from WT ($n = 10$) and KO ($n = 14$) mice ($p < 0.0001$ for all odorants tested). ***B***, Response to 0.1 M heptanal from endoturbinates 2, 2b, 3, and 4 from WT ($n = 5$) and KO ($n = 7$) mice. The recordings were made from 12 points on each turbinate (right, graphical representation on the epithelium). WT and KO data are significantly different ($p < 0.05$), except for positions 4 and 10 on T4. Error bars represent SE.

tified (Huang et al., 1999; Kulaga et al., 2004; McEwen et al., 2007; Kerr et al., 2008) but their role in olfactory transduction remained unaddressed.

Gγ13 is expressed in multiple tissues including cortical neurons (Huang et al., 1999). To avoid possible complications from altered functions of other organs, we decided to generate a mouse line with the two *Gng13* coding exons floxed to conditionally ablate this gene (Fig. 1), as it has been recently done with another chemosensory G-protein subunit Gαo (Chamero et al., 2011). Crossing this mouse with another gene knock-in mouse that expresses Cre-recombinase under the *Omp* promoter limited the excision of *Gng13* to the OMP-expressing OSNs(Li et al., 2004), resulting in a complete loss of Gγ13 immunoreactivity in the olfactory epithelium of the knock-out mice ($Gng13^{-/-}$) (Fig. 2). Gγ13 immunoreactivity was also absent in most of the axonal bundles beneath the epithelium except those in the middle (Fig. 2*H*). Western blot and quantitative real-time PCR analyses showed that Gγ13 protein and its transcript were much reduced in KO olfactory epithelium (Fig. 3). Those results indicate that the nullification of Gγ13 expression in OSNs was successful and that the remaining immunoreactive bundles may contain axons from other Gγ13-expressing neurons than OSNs.

As suggested in previous biochemical studies, Gγ13 may interact with Gαolf, Gβ1, Ric-8B, and CEP290 *in vitro* (McEwen et al., 2007; Kerr et al., 2008). Thus, we also investigated the effect of *Gng13*-KO on the expression of these proteins. Immunohistochemistry found a very similar loss of expression of both the Gαolf, and Gβ1 subunits as for the γ subunit in the olfactory epithelium of the $Gng13^{-/-}$ mice (Fig. 2*C*,*D*,*J*,*K*). In contrast, the expression of another olfactory signaling protein, ACIII, seemed strong although the subcellular distribution appeared to have shifted to the cell body

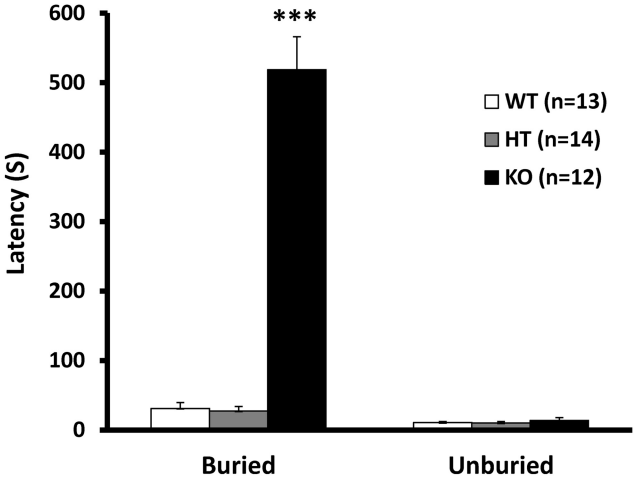

Figure 7. *Gng13*-KO mice showed significantly impaired food-seeking capabilities. KO mice took significantly longer to locate a 1 g chow pellet, scented with 5 μl of 10% peanut butter, buried under the bedding compared with heterozygous (HT) or WT littermates. However, all three types of mice located food placed on top of the bedding in similarly short times. Values are means ±SE. ***$p < 0.001$.

(Fig. 2*E*,*L*). The cilia layer was present in KO epithelium because the immunosignal of acetylated tubulin was robust, so was that of OMP (Fig. 2). Western blot analysis (Fig. 3*A*,*B*) showed that the proteins of Gγ13, Gβ1, Ric-8B, and CEP290 were markedly diminished in KO sample, suggesting that these proteins' production and/or stability was reduced. Real-time PCR data also indicated that the transcripts for Gγ13, Gαolf, and Gβ1 were also significantly less in KO sample (Fig. 3*C*), indicating that these genes' transcription was also destabilized. Interestingly, the transcription of OMP seemed to be affected as well, and the underlying mechanism, however, has yet to be revealed. One possibility is that the number of mature OSNs might have been reduced in KO olfactory epithelium due to accelerated cell turnover.

Previous studies on the assembly and trafficking of heterotrimeric G-proteins indicate that the nascent Gβ and Gγ subunits, in the presence of accessory chaperone proteins, first form a heterodimer, and then form a heterotrimer with a Gα subunit, and the heterotrimer Gαβγ is then delivered to the lipid raft on the plasma membrane where the receptor resides (Marrari et al., 2007). Upon dimerization, G-protein β and γ subunits do not dissociate under normal conditions (Simonds et al., 1991). In this study, the absence of Gβ1 and Gαolf subunits in the *Gng13*$^{-/-}$ olfactory epithelium strongly indicates that the lack of Gγ subunits lead to no formation of any Gβγ dimers with Gβ1 or Gαβγ trimers with Gαolf, triggering the rapid degradation of Gαolf and Gβ proteins in OSNs. This same consequence has been observed in the retina where the rod-specific transducin Gαt and Gβ1 were lost in the photoreceptors when Gγ1 gene was nullified (Lobanova et al., 2008; Kolesnikov et al., 2011). In addition to Gγ13, the deletion of *Gng7* gene in medium-sized neurons in the caudate-putamen in the striatum also caused an analogous loss of Gαolf in these neurons (Schwindinger et al., 2003), suggesting that Gαolf can interact with different Gβγ subunits. But in OSNs, our results demonstrate that Gαolf exclusively partners with Gβ1γ13 because both Gαolf and Gβ1 were eliminated from the olfactory epithelium, and that no other G-protein γ subunits, e.g., Gγ8, can compensate the role of Gγ13 in OSNs, forming functional Gβγ dimers or Gαβγ trimers with Gβ1 and Gαolf.

Interestingly, in OSNs, the requirement of co-occurrence of two proteins for correct protein assembly and trafficking is not limited to the heterotrimeric G-proteins. Knock-out of either of the heterotrimeric CNG channel's auxiliary subunits A4 and B1b resulted in loss of the other subunit in OSNs (Michalakis et al., 2006). Our data showed that the expression of another downstream signaling protein ACIII, however, seemed to be strong in the *Gng13*$^{-/-}$ cilia layer (Fig. 2*E*,*L*), indicating that its expression and sorting is not directly linked to those of the G-protein subunits.

Investigations of the electrophysiological responses of the *Gng13*$^{-/-}$ olfactory epithelium revealed widespread deficits to a broad range of odorants, including three presumable pheromones. Regardless of odorants tested or turbinal positions recorded from, Gγ13 knock-out mice showed much reduced EOG responses across the entire olfactory epithelium (Figs. 5,6). This is similar to the responses observed in Gαolf knock-out mice (Belluscio et al., 1998), indicating that the abolishment of either of the two G-protein subunits eliminates the G-protein-mediated olfactory signal transduction in OSNs.

Odor-guided behavioral studies showed that Gγ13 knock-out mice required significantly longer time to locate buried food but nearly the same time to find the unburied food as did the WT or heterozygous control mice (Fig. 7). These data were in full agreement with the aforementioned molecular and electrophysiological data, confirming that the KO mice were anosmic and unable to perform an odorant-guided task, but able to use other sensory inputs to finish the task as well as control mice. The profound effect of the KO on the behavioral responses is comparable with those of the mice deficient in other olfactory signaling components, such as systematic ablation of ACIII, Gαolf or CNGA2 (Brunet et al., 1996; Belluscio et al., 1998; Wong et al., 2000), but appears more severe than those of other proteins expressed in OSNs, including the systematic knock-out of OMP or olfactory tissue-specific knock-out of NCXK4 (Buiakova et al., 1996; Stephan et al., 2012).

In addition to Gβ1 and Gαolf, Gγ13 in OSNs may also interact with other proteins, and perform other functions, including gene expression regulation (DeMaria and Ngai, 2010). Recent studies have shown that Gγ13 can physically bind to α-gustducin, Gβ3, Ric-8B, and PDZ domain-containing proteins (Huang et al., 1999; Blake et al., 2001; Li et al., 2006; Kerr et al., 2008; Liu et al., 2012). Gγ13 occurs in the OSN axonal termini as well and *Gng13* KO seemed to have some impact on the glomerular structure (Fig. 4). Because α-gustducin, Gαolf, or Gβ1 is absent in the axonal termini, it is currently unknown what functions Gγ13 exerts in these termini although it may possibly interact with other yet-to-be-identified G-protein subunits or PDZ-domain-containing proteins in organizing axon terminal structures in the context of glomerulus in the olfactory bulb.

In conclusion, we have conditionally nullified the expression of Gγ13 in OMP-expressing OSNs, and the mutant mice displayed severe physiological and behavioral anosmia. The *Gng13* gene knock-out abolished expression of not only Gγ13 but also Gβ1 and Gαolf, as well as Ric-8B and CEP290 in OSNs, indicating that Gβ1 and Gγ13 are the exclusive βγ partners of Gαolf, and Ric-8B and CEP290 are important interacting proteins in the olfactory epithelium. Further studies are needed to identify the target effectors that Gβ1γ13 dimers act on in OSNs, as well as Gγ13's interacting proteins in the axonal termini of OSNs.

References

Bakalyar HA, Reed RR (1990) Identification of a specialized adenylyl cyclase that may mediate odorant detection. Science 250:1403–1406. CrossRef Medline

Belluscio L, Gold GH, Nemes A, Axel R (1998) Mice deficient in G_{olf} are anosmic. Neuron 20:69–81. CrossRef Medline

Billig GM, Pál B, Fidzinski P, Jentsch TJ (2011) Ca^{2+}-activated Cl^- currents are dispensable for olfaction. Nat Neurosci 14:763–769. CrossRef Medline

Blake BL, Wing MR, Zhou JY, Lei Q, Hillmann JR, Behe CI, Morris RA, Harden TK, Bayliss DA, Miller RJ, Siderovski DP (2001) G beta association and effector interaction selectivities of the divergent G gamma subunit G gamma(13). J Biol Chem 276:49267–49274. CrossRef Medline

Bönigk W, Bradley J, Müller F, Sesti F, Boekhoff I, Ronnett GV, Kaupp UB, Frings S (1999) The native rat olfactory cyclic nucleotide-gated channel is composed of three distinct subunits. J Neurosci 19:5332–5347. Medline

Bradley J, Li J, Davidson N, Lester HA, Zinn K (1994) Heteromeric olfactory cyclic nucleotide-gated channels: a subunit that confers increased sensitivity to cAMP. Proc Natl Acad Sci U S A 91:8890–8894. CrossRef Medline

Brunet LJ, Gold GH, Ngai J (1996) General anosmia caused by a targeted disruption of the mouse olfactory cyclic nucleotide-gated cation channel. Neuron 17:681–693. CrossRef Medline

Buck L, Axel R (1991) A novel multigene family may encode odorant receptors: a molecular basis for odor recognition. Cell 65:175–187. CrossRef Medline

Buiakova OI, Baker H, Scott JW, Farbman A, Kream R, Grillo M, Franzen L, Richman M, Davis LM, Abbondanzo S, Stewart CL, Margolis FL (1996) Olfactory marker protein (OMP) gene deletion causes altered physiological activity of olfactory sensory neurons. Proc Natl Acad Sci U S A 93:9858–9863. CrossRef Medline

Chamero P, Katsoulidou V, Hendrix P, Bufe B, Roberts R, Matsunami H, Abramowitz J, Birnbaumer L, Zufall F, Leinders-Zufall T (2011) G protein G(alpha)o is essential for vomeronasal function and aggressive behavior in mice. Proc Natl Acad Sci U S A 108:12898–12903. CrossRef Medline

Cygnar KD, Stephan AB, Zhao H (2010) Analyzing responses of mouse olfactory sensory neurons using the air-phase electroolfactogram recording. J Vis Exp 37:1850. CrossRef Medline

DeMaria S, Ngai J (2010) The cell biology of smell. J Cell Biol 191:443–452. CrossRef Medline

Dhallan RS, Yau KW, Schrader KA, Reed RR (1990) Primary structure and functional expression of a cyclic nucleotide-activated channel from olfactory neurons. Nature 347:184–187. CrossRef Medline

Dupr é DJ, Robitaille M, Rebois RV, Hébert TE (2009) The role of Gbetagamma subunits in the organization, assembly, and function of GPCR signaling complexes. Annu Rev Pharmacol Toxicol 49:31–56. CrossRef Medline

Glusman G, Yanai I, Rubin I, Lancet D (2001) The complete human olfactory subgenome. Genome Res 11:685–702. CrossRef Medline

Huang L, Shanker YG, Dubauskaite J, Zheng JZ, Yan W, Rosenzweig S, Spielman AI, Max M, Margolskee RF (1999) Ggamma13 colocalizes with gustducin in taste receptor cells and mediates IP3 responses to bitter denatonium. Nat Neurosci 2:1055–1062. CrossRef Medline

Jiang P, Song J, Gu G, Slonimsky E, Li E, Rosenthal N (2002) Targeted deletion of the MLC1f/3f downstream enhancer results in precocious MLC expression and mesoderm ablation. Dev Biol 243:281–293. CrossRef Medline

Jones DT, Reed RR (1989) Golf: an olfactory neuron specific-G protein involved in odorant signal transduction. Science 244:790–795. CrossRef Medline

Kerr DS, Von Dannecker LE, Davalos M, Michaloski JS, Malnic B (2008) Ric-8B interacts with G alpha olf and G gamma 13 and co-localizes with G alpha olf, G beta 1 and G gamma 13 in the cilia of olfactory sensory neurons. Mol Cell Neurosci 38:341–348. CrossRef Medline

Kleene SJ (1993) Origin of the chloride current in olfactory transduction. Neuron 11:123–132. CrossRef Medline

Kolesnikov AV, Rikimaru L, Hennig AK, Lukasiewicz PD, Fliesler SJ, Govardovskii VI, Kefalov VJ, Kisselev OG (2011) G-protein betagamma-complex is crucial for efficient signal amplification in vision. J Neurosci 31:8067–8077. CrossRef Medline

Kulaga HM, Leitch CC, Eichers ER, Badano JL, Lesemann A, Hoskins BE, Lupski JR, Beales PL, Reed RR, Katsanis N (2004) Loss of BBS proteins causes anosmia in humans and defects in olfactory cilia structure and function in the mouse. Nat Genet 36:994–998. CrossRef Medline

Kwon HJ, Koo JH, Zufall F, Leinders-Zufall T, Margolis FL (2009) Ca extrusion by NCX is compromised in olfactory sensory neurons of OMP mice. PLoS One 4:e4260. CrossRef Medline

Lee AC, He J, Ma M (2011) Olfactory marker protein is critical for functional maturation of olfactory sensory neurons and development of mother preference. J Neurosci 31:2974–2982. CrossRef Medline

Li J, Ishii T, Feinstein P, Mombaerts P (2004) Odorant receptor gene choice is reset by nuclear transfer from mouse olfactory sensory neurons. Nature 428:393–399. CrossRef Medline

Li Z, Benard O, Margolskee RF (2006) Ggamma13 interacts with PDZ domain-containing proteins. J Biol Chem 281:11066–11073. CrossRef Medline

Liman ER, Buck LB (1994) A second subunit of the olfactory cyclic nucleotide-gated channel confers high sensitivity to cAMP. Neuron 13:611–621. CrossRef Medline

Liu P, Jenkins NA, Copeland NG (2003) A highly efficient recombineering-based method for generating conditional knock-out mutations. Genome Res 13:476–484. CrossRef Medline

Liu Z, Fenech C, Cadiou H, Grall S, Tili E, Laugerette F, Wiencis A, Grosmaitre X, Montmayeur JP (2012) Identification of new binding partners of the chemosensory signaling protein Gγ13 expressed in taste and olfactory sensory cells. Front Cell Neurosci 6:26. CrossRef Medline

Lobanova ES, Finkelstein S, Herrmann R, Chen YM, Kessler C, Michaud NA, Trieu LH, Strissel KJ, Burns ME, Arshavsky VY (2008) Transducin gamma-subunit sets expression levels of alpha- and beta-subunits and is crucial for rod viability. J Neurosci 28:3510–3520. CrossRef Medline

Lowe G, Gold GH (1993) Nonlinear amplification by calcium-dependent chloride channels in olfactory receptor cells. Nature 366:283–286. CrossRef Medline

Luo AH, Cannon EH, Wekesa KS, Lyman RF, Vandenbergh JG, Anholt RR (2002) Impaired olfactory behavior in mice deficient in the alpha subunit of G(o). Brain Res 941:62–71. CrossRef Medline

Ma M (2010) Multiple olfactory subsystems convey various sensory signals. In: The Neurobiology of Olfaction (Menini A, ed). Boca Raton, FL:CRC.

Marrari Y, Crouthamel M, Irannejad R, Wedegaertner PB (2007) Assembly and trafficking of heterotrimeric G proteins. Biochemistry 46:7665–7677. CrossRef Medline

McEwen DP, Koenekoop RK, Khanna H, Jenkins PM, Lopez I, Swaroop A, Martens JR (2007) Hypomorphic CEP290/NPHP6 mutations result in anosmia caused by the selective loss of G proteins in cilia of olfactory sensory neurons. Proc Natl Acad Sci U S A 104:15917–15922. CrossRef Medline

Michalakis S, Reisert J, Geiger H, Wetzel C, Zong X, Bradley J, Spehr M, Hüttl S, Gerstner A, Pfeifer A, Hatt H, Yau KW, Biel M (2006) Loss of CNGB1 protein leads to olfactory dysfunction and subciliary cyclic nucleotide-gated channel trapping. J Biol Chem 281:35156–35166. CrossRef Medline

Mombaerts P (2004) Genes and ligands for odorant, vomeronasal and taste receptors. Nat Rev Neurosci 5:263–278. CrossRef Medline

Munger SD, Lane AP, Zhong H, Leinders-Zufall T, Yau KW, Zufall F, Reed RR (2001) Central role of the CNGA4 channel subunit in Ca^{2+}-calmodulin-dependent odor adaptation. Science 294:2172–2175. CrossRef Medline

Munger SD, Leinders-Zufall T, Zufall F (2009) Subsystem organization of the mammalian sense of smell. Annu Rev Physiol 71:115–140. CrossRef Medline

Okano M, Takagi SF (1974) Secretion and electrogenesis of the supporting cell in the olfactory epithelium. J Physiol 242:353–370. Medline

Ottoson D (1956) Analysis of the electrical activity of the olfactory epithelium. Acta Physiol Scand Suppl 35:1–83. Medline

Reisert J, Yau KW, Margolis FL (2007) Olfactory marker protein modulates the cAMP kinetics of the odour-induced response in cilia of mouse olfactory receptor neurons. J Physiol 585:731–740. CrossRef Medline

Rodriguez I, Boehm U (2009) Pheromone sensing in mice. Results Probl Cell Differ 47:77–96. CrossRef Medline

Schwindinger WF, Betz KS, Giger KE, Sabol A, Bronson SK, Robishaw JD (2003) Loss of G protein gamma 7 alters behavior and reduces striatal

alpha(olf) level and cAMP production. J Biol Chem 278:6575–6579. CrossRef Medline

Simonds WF, Butrynski JE, Gautam N, Unson CG, Spiegel AM (1991) G-protein beta gamma dimers: membrane targeting requires subunit coexpression and intact gamma C-A-A-X domain. J Biol Chem 266:5363–5366. Medline

Spiegelberg BD, Hamm HE (2005) G betagamma binds histone deacetylase 5 (HDAC5) and inhibits its transcriptional co-repression activity. J Biol Chem 280:41769–41776. CrossRef Medline

Stephan AB, Shum EY, Hirsh S, Cygnar KD, Reisert J, Zhao H (2009) ANO2 is the cilial calcium-activated chloride channel that may mediate olfactory amplification. Proc Natl Acad Sci U S A 106:11776–11781. CrossRef Medline

Stephan AB, Tobochnik S, Dibattista M, Wall CM, Reisert J, Zhao H (2012) The Na^+/Ca^{2+} exchanger NCKX4 governs termination and adaptation of the mammalian olfactory response. Nat Neurosci 15:131–137. CrossRef Medline

Tirindelli R, Ryba NJ (1996) The G-protein gamma-subunit G gamma 8 is expressed in the developing axons of olfactory and vomeronasal neurons. Eur J Neurosci 8:2388–2398. CrossRef Medline

Wang H, Zhou M, Brand J, Huang L (2007) Inflammation activates the interferon signaling pathways in taste bud cells. J Neurosci 27:10703–10713. CrossRef Medline

Wong ST, Trinh K, Hacker B, Chan GC, Lowe G, Gaggar A, Xia Z, Gold GH, Storm DR (2000) Disruption of the type III adenylyl cyclase gene leads to peripheral and behavioral anosmia in transgenic mice. Neuron 27:487–497. CrossRef Medline

Yang M, Crawley JN (2009) Simple behavioral assessment of mouse olfaction. Curr Protoc Neurosci 8:24. CrossRef Medline

Young JM, Friedman C, Williams EM, Ross JA, Tonnes-Priddy L, Trask BJ (2002) Different evolutionary processes shaped the mouse and human olfactory receptor gene families. Hum Mol Genet 11:535–546. CrossRef Medline

Youngentob SL, Margolis FL (1999) OMP gene deletion causes an elevation in behavioral threshold sensitivity. Neuroreport 10:15–19. CrossRef Medline

Youngentob SL, Margolis FL, Youngentob LM (2001) OMP gene deletion results in an alteration in odorant quality perception. Behav Neurosci 115:626–631. CrossRef Medline

Zhang X, Firestein S (2002) The olfactory receptor gene superfamily of the mouse. Nat Neurosci 5:124–133. CrossRef Medline